MODELLING RECOVERY AND RECRYSTALLIZATION, APPLIED TO BACK-ANNEALING OF ALUMINIUM SHEET ALLOYS

Jan Anders SÆTER*, Børge FORBORD*, Hans Erik VATNE and Erik NES***

*Department of Metallurgy, Norwegian University of Science and Technology, N-7034 Trondheim, Norway

**Hydro Aluminium, R&D Center Sunndasløra, N-6600 Sunndalsøra, Norway

ABSTRACT Recovery of mechanical properties during annealing of deformed metals has been modelled based on a microstructural representation comprising two elements, (i) the cell/subgrain structure (size δ) and (ii) the dislocation density (ρ_i) within the subgrains. These two microstructural elements are treated as independent variables which during annealing define the flow stress $\sigma(T,t)$ as follows:

$$\sigma(T,t) = \sigma_i + (1 - X(T,t))\left\{\alpha_1 MGb\sqrt{\rho_i(T,t)} + \alpha_2 MGb / \delta(T,t)\right\}$$

Where $X(T,t)$ is the volume fraction recrystallized. The recovery reaction has been modelled in terms of solute pinning of migrating dislocations and sub-boundaries. The annealing out of dislocations has been analysed as a thermally activated glide reaction. Subgrain growth is treated analogous to normal grain growth, i.e. as a reaction controlled by sub-boundary migration. Recrystallization kinetics is modelled in terms of simple Avrami kinetics.

1 INTRODUCTION

The microstructural changes which occur upon annealing of a deformed metal are commonly described in terms of recovery and recrystallization. The magnitude of the recovery contribution to the softening reaction will depend on the rate of recovery as compared to the nucleation and growth rate of recrystallization. Two extreme cases are illustrated by the softening curves shown in Fig. 1. Figure 1a, based on work by Cook and Richards [1], shows the normalised residual strain hardening, R, plotted against time of isothermal annealing of cold deformed high purity copper at low temperatures. (For a definition of R, see Eq. 2). It is obvious that recovery plays no role in this transformation. For aluminium (Fig. 1b), however, a substantial proportion of the stored energy is consumed by recovery, (the arrows indicate the first visible signs of recrystallization, from Furu, Ørsund and Nes [2]). It is obvious that in the latter case recovery cannot be ignored in the modelling of the softening reaction.

In the following, recovery will be discussed in terms of its effect on mechanical properties and in this context a most notable characteristic is the logarithmic decay in properties as illustrated in Figs. 1b and 2. This property-time relationship seems to apply to many metals, whether single or polycrystals, high purity metals or commercial grades, deformed a few percent or subjected to heavy rolling or other modes of deformation prior to annealing. A case of special interest is recovery in AlMg-alloys. Strain hardened AlMg-alloys recover much more rapidly than other wrought aluminium alloys. Further, in AlMg-alloys, recovery can even be followed at room temperature. The classic experiment in this context is the one performed over nearly two decades by Alcoa Laboratory through the 1930s and 1940s [3,4]. Some of these results are collected in Fig. 2 a-c, which illustrates the recovery of the yield strength of alloys containing 2.4 wt%, 4 wt% and 6 wt%.

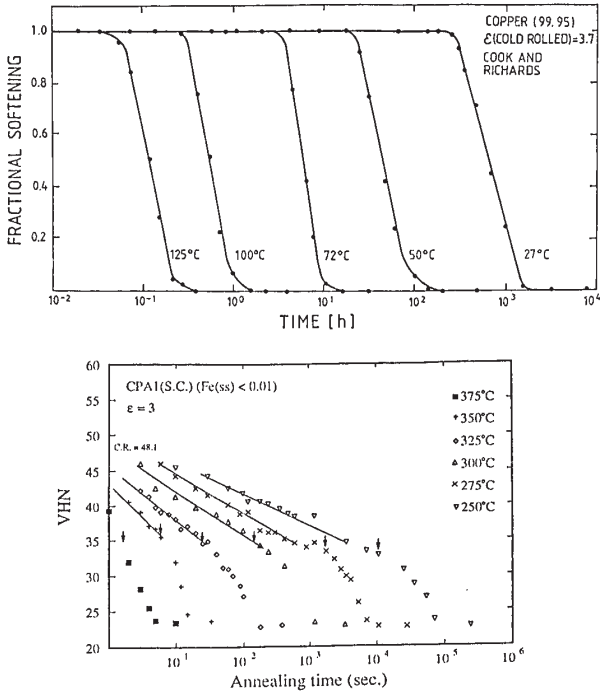

Fig. 1. Fractional residual strain hardening curves and hardness curves for isothermal annealing of a) copper, rolling strain 3.7 [1], and b) commercial purity aluminium, rolling strain 3 [2].

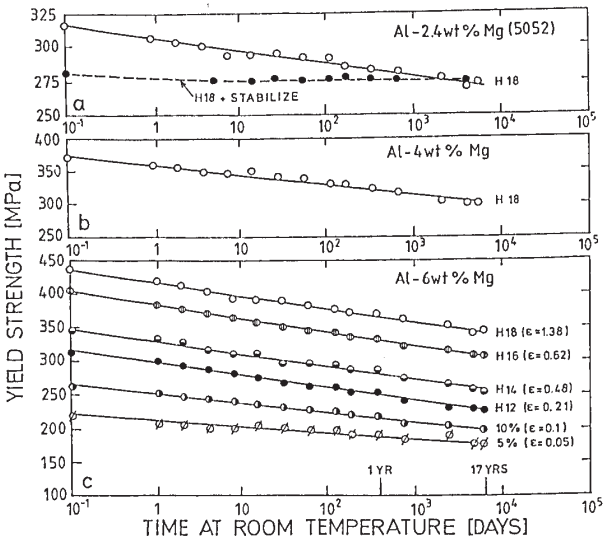

Fig. 2. Variation in yield stress as a function of time at room temperature for the AlMg alloys given [4].

Recovery of mechanical properties during annealing of deformed metals has recently been modelled by Nes [5], Furu et al. [2] and Nes and Sæter [6] on the basis of a microstructural representation comprising two elements, (i) the cell/subgrain structure (size δ) and the dislocation density (ρ_i) within the subgrains. These two microstructural elements were treated as independent variables and the recovery of flow stress obtained by adding the time dependent contributions due to subgrain growth and dislocation network growth as follows:

$$\sigma(T,t) = \sigma_i + \alpha_1 MGb\sqrt{\rho_i(T,t)} + \alpha_2 MGb / \delta(T,t) \qquad (1)$$

Or in terms of the normalised fractional residual strain hardening, R:

$$R = \frac{\sigma(T,t) - \sigma_i}{\sigma_0 - \sigma_i} = f\sqrt{\frac{\rho_i(T,t)}{\rho_{i0}}} + (1-f)\frac{\delta_0}{\delta(T,t)} \qquad (2)$$

Where $f = \alpha_1 MGb\sqrt{\rho_o}/(\sigma_o - \sigma_i)$. σ_o, ρ_{io} and δ_o are the flow stress, the dislocation density and average cell size at time $t=0$ respectively. G is the shear modulus, b is the Burgers vector, M is the Taylor factor, σ_i is the friction stress and α_1 and α_2 are constants. It follows that f and $(1-f)$ are the fractional contribution to the recoverable flow stress prior to annealing due to the distributed dislocations and subgrain structure, respectively.

Equation 1 applies only as long as the effect of recrystallization can be ignored. If, however, at a given time and temperature, a volume fraction $X(T,t)$ has recrystallized, then Eq. 1 needs to be rewritten on the form

$$\sigma(T,t) = \sigma_i + (1 - X(T,t))\left[\alpha_1 MGb\sqrt{\rho_i(T,t)} + \alpha_2 MGb\frac{1}{\delta(T,t)}\right] \qquad (3)$$

This approach to the modelling of recovery and recrystallization will in the following be briefly reviewed and further developed with the specific objective in mind of designing models capable of handling industrial back annealing of sheet alloys. In this treatment emphasis will be on the modelling of the recovery reactions. Recrystalization is handled in a simple parametric way in terms of standard Avrami kinetics.

2 MODEL

As pointed out above, this model rests on the assumption that recovery can be analysed in terms of a microstructural representation comprising two elements; the cell/subgrain size (δ) and the dislocation density inside the subgrains (ρ_i). In previous works by the present group [2,5,6] indirect support for this approach has been presented, for instance, results reported by Young et al. [7] has been interpreted in this context. Young et al. deformed high purity aluminium to strains of 5%, 10%, 15% and 20% (tensile deformation). The cell diameter was measured in TEM and the flow stress was found to scale with $1/\delta$ as illustrated in the log-log-plot in Fig. 3. The tensile deformation experiments were followed by static annealing for 300 hours at three different temperatures (120°C, 160°C and 200°C). Microstructural investigation in TEM revealed that at the lowest temperature no subgrain growth could be detected while at the higher temperatures small increases in the subgrain sizes were recorded. The most salient change resulting from the recovery treatment was a transformation of the cell boundaries into sharp sub-boundaries. As shown in Fig. 3 a significant drop in flow stress was observed as a result of the annealing treatments.

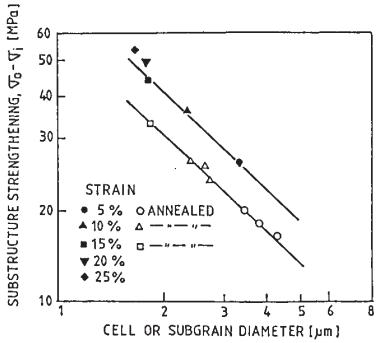

Fig. 3. The effects of various pre-strains on substructure strengthening, as deformed and after annealing, for details see the text. From Young et al. [7].

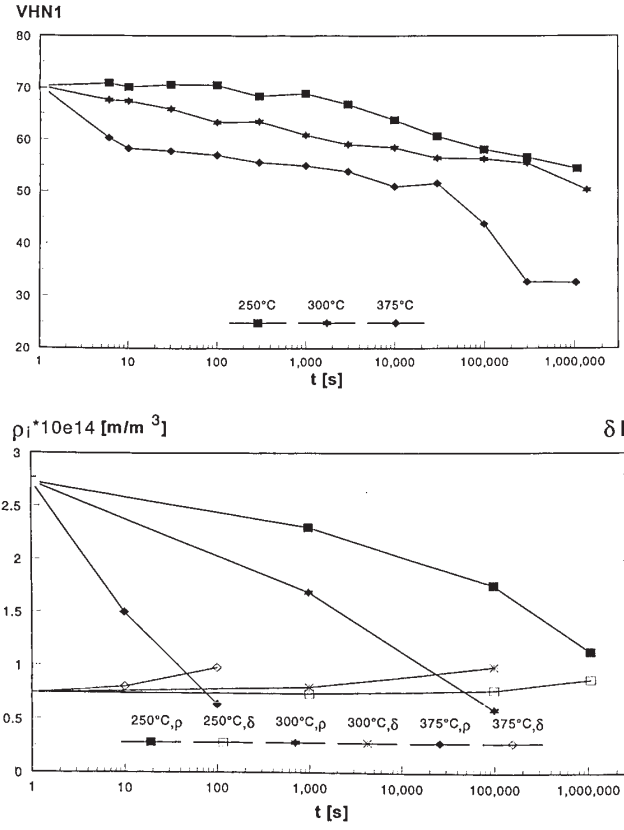

Fig. 4. a) Variation in hardness as a function of time at the temperatures given. b) Corresponding variation in dislocation density, ρ_i, and subgrain size, δ.

These drops in yield stress were modelled by Nes and Sæter [6] as being the result of the annealing out of the dislocations in the cell interior. The annealing behaviour of such dislocations was not studied by Young et al., and their interpretation was built upon the assumption that the recovery of cell boundary dislocations was responsible for the flow stress changes. Figure 4, however, taken from a recent work by Forbord [8] provides direct evidence for the present microstructural picture. Forbord has studied in great detail the annealing behaviour of an AlMn0.5 alloy, cold rolled to a strain of 2 prior to annealing at the temperatures indicated in the figure. Note that an appreciable reduction in the hardness can be attributed exclusively to the annealing out of the dislocations located within subgrains.

2.1 Annealing out of dislocations

The recovery of dislocations due to network growth is commonly treated [9-11] as follows: If r is the average distance between dislocations in the network its time dependence can be written:

$$\frac{dr}{dt} = m\frac{\Gamma}{r} \tag{4}$$

Where Γ is the line tension and m the dislocation mobility. This expression is derived on the assumption that m is a constant (at a constant temperature). However, $v = mF$ (where v is the dislocation speed and F is the force per unit length acting on the dislocation) is valid only for relatively small values of F. In general the migration speed will be given by:

$$v = \nu_D l_g B_a (\exp - \frac{U_a}{kT}) 2 \sinh \frac{Fl_a b}{kT} \tag{5}$$

Where ν_D is a frequency term, U_a an activation energy, l_a an activation length (i.e. the dislocation length involved in each thermal activation) l_g is the distance travelled in between thermal activations, k is Boltzmann's constant and T the annealing temperature. In the special cases where $Fl_a b/kT << 1$, Eq. 5 is reduced to the form of Eq. 4. Accordingly, as the value of $Fl_a b/kT$ not necessarily needs to be smaller than one in a network growth situation, Eq. 4 will be replaced by :

$$\frac{dr}{dt} = C_1 v \tag{6}$$

Where C_1 is a constant which in this modelling treatment needs to be determined experimentally and v is the average migration rate of the dislocations, given by Eq. 8. This average speed is due to a force per unit length which can be derived from the free energy change associated with the decrease in dislocation density, i.e.

$$F = \alpha_3 G b^2 / r = \alpha_3 G b^3 \sqrt{\rho_i} \tag{7}$$

Where α_3 is a constant of order unity.

The dislocation network may expand due to recombination or annihilation reactions of different kinds as discussed in Refs. 5 and 6. In commercial aluminium alloys thermally activated glide has been identified as the rate controlling reaction [5], i.e. the dragging of jogs on screw dislocations, in which case $l_a = l_j$ where l_j is the jog separation. In pure metals, jogs which are formed due to intersection with forest dislocations, may easily disappear due to lateral drift and

subsequent annihilation due to recombination with other jogs. Balancing the jog creation rate with the annihilation rate gives a steady state jog density, which will scale with the density of stored dislocations (see Ref. 5). In solute containing alloys, lateral drift of jogs will be inhibited by the solute atoms, a consequence of which is that the jog density may be determined by the solute concentration. In the case of solute pinning, U_a can be replaced by U_s (activation energy of solute diffusion). It follows that in a situation where network growth is controlled by thermally activated glide (jogs contaminated by solute atoms) Eq. 6 can be written on the form:

$$\frac{d\rho_i}{dt} = -\nu_D B_\rho l_g \rho_i^{3/2} (\exp - \frac{U_s}{kT})(2\sinh \frac{Gb^3 l_j \sqrt{\rho_i}}{kT}) \tag{8}$$

Where $B_\rho = 2\, B_a\, C_1$ and α_3 is defined as being equal to unity.

Equation 8 cannot be solved analytically, but numerical solutions are easily derived. Approximate solutions can be obtained for the following two cases determined by the value of the ratio; Fl_jb/kT.

$Fl_jb/kT>1$:

$$\sqrt{\frac{\rho_i}{\rho_{i0}}} = 1 - \frac{1}{l_j\sqrt{\rho_{i0}}}(\frac{kT}{Gb^3})\ln(1+\frac{t}{\tau_1}) \tag{9}$$

where

$$\tau_1 = \left[\nu_D \rho_{i0} l_g l_j B_\rho (\frac{Gb^3}{kT}) \exp - (\frac{U_s - l_j\sqrt{\rho_{i0}} Gb^3}{kT})\right]^{-1}$$

$Fl_jb/kT<<1$:

$$\sqrt{\frac{\rho_i}{\rho_{i0}}} = (1+\frac{t}{\tau_2})^{1/2} \tag{10}$$

where

$$\tau_2 = \left[\nu_D \rho_{i0} l_j l_g B_\rho (\frac{Gb^3}{kT}) \exp - \frac{U_s}{kT}\right]^{-1}$$

Regarding the effect of solute atoms on the jog density, l_j^{-1}; different situations will arise depending on the density of stored dislocations prior to annealing or the amount of cold deformation prior to annealing. In a situation where the lateral drift of jogs is controlled by solute atoms the solute content will control the jog separation provided the accumulated density of jogs defines a jog spacing which is equal to or less that of the solute atoms. In the absence of lateral drift, the accumulated jog density is, for a given cold deformation, defined by the slip length $L = C/\sqrt{\rho}$, i.e. $l_j = \omega_j/(C\sqrt{\rho})$, where the slip length parameter C typically has a value of 100, ω_j is a geometric constant which needs to be determined experimentally and ρ is the total dislocation density. The total dislocation density can be expressed in various ways: At relatively small strains (stage II) the

principle of scaling (similitude) is expected to apply and $\sqrt{\rho}=\sqrt{\rho_i}/f_{sc}$ where f_{sc} is a constant which is equal to f (see Eq. 2). At large strains the principle of scaling no longer applies, and the total dislocation density becomes $\rho=\rho_i+3b\varphi/\delta$ (φ is the sub- boundary misorientation, for more details see Ref. 6). And it follows that if $\omega_j/(C\sqrt{\rho_0}) < l_s$, then a natural consequence of lateral drift becomes that

$$l_j = l_s = \omega_s b c^{-e} \tag{11}$$

where ω_s is a geometric constant and the exponent e is expected to have a value in the range $0.5 < e < 1$. If $\omega_j/C\sqrt{\rho_o} > l_s$ then;

$$l_j = \omega_j / C\sqrt{\rho_0} \tag{12}$$

2.2 Subgrain growth

Subgrain growth has been attributed to either one of two distinctly different mechanisms: (i) subgrain coalescence or (ii) migration of sub-boundaries. The first theory of subgrain growth due to boundary coalescence was presented by Li [10] with some later refinements due to Sandström [11] and Doherty and Szpunar [12]. There is no doubt that coalescence may occur as isolated events especially associated with sub-boundaries located in the vicinity of high-angle boundaries [13, 14]. Further, during annealing of lightly deformed metals where cell/subgrain boundaries are of low misorientation (typically 0.5°), coarsening due to coalescence as the dominating mechanism has been reported by Young et al. [7]. However, during annealing of heavily deformed metals no convincing evidence has been reported in support of that coalescence plays any significant role in subgrain growth under conditions where substantial coarsening is observed. To the contrary, based on a detailed in situ TEM-examination of subgrain coarsening in an Al 0.46 wt%Cu alloy, Gleiter [15] concluded that the reaction was analogous to the process of grain growth in a polycrystal, i.e. by migration of sub-boundaries. Gleiter did, however, report some evidence of boundary dissolution during migration. He observed that boundaries with dislocation densities less than $2\cdot10^7$ m^{-1} (or a misorientation less than 0.3 degrees) could emit dislocations during the migration process, while for all boundaries which had a higher dislocation density (the majority of boundaries) this process was not observed. Gleiter specifically noted that the sub-boundaries moved by a ledge mechanism and a dislocation model for this pattern of migration was presented.

Sandström et al. [13, 16] have studied subgrain growth in high purity aluminium and an AlMn alloy. Several coarsening mechanisms were observed including various types of coalescence reactions. However, at temperatures above 200°C, growth due to boundary migration was found to be the dominating mechanism. At lower temperatures the observed coarsening appeared to be due to coalescence, a reaction which rapidly leveled off, resulting in only a minor increase in subgrain size (from 0.75 μm to 0.9 μm, for details see Sandstöm et al. [13]).

Subgrain growth kinetics. Furu et al. [2] modelled subgrain growth based on a rate equation similar to Eq. 6 (where r now has the meaning subgrain radius). This treatments is similar to that of Sandström [16] in the sense that the reaction is treated analogously to that of normal grain growth with the migration of sub-boundary dislocations being the rate controlling reaction. However, the Furu et al. analysis is based on using Eq. 5 for the dislocation speed, while Sandström limited his analysis to the special solution of Eq. 5 corresponding to $Fl_ab<<kT$. i.e. a pure climb analysis. The model assumes that the sub-boundary energy can be approximated by using the Read-Shockley equation: $\gamma_{sb}=\alpha_4 Gb\varphi\ln(e\varphi_c/\varphi)$ where φ is the boundary misorientation, $\alpha_4=1/4\pi(1-\nu) \approx 0.1$ for an elementary tilt boundary and ν is the Poisson's ratio. φ_c is the angle at which the boundary will

have maximum energy, a common estimate for φ_c is 15°. A typical φ-value is 3°, i.e. $\gamma_{sb}=0.02Gb$. Further, the driving pressure for subgraing growth is typically of the size P = $2\gamma_{sb}/\delta$ or $P\approx 0.04Gb/\delta$. And it follows that in the case of subgrain growth by boundary migration the rate equation (Eq. 6) takes the form

$$\frac{d\delta}{dt} = v_D B_\delta b(\exp-\frac{U_a}{kT})2\sinh\frac{PV_a}{kT} \qquad (13)$$

Where V_a is an activation volume. Two cases of diffusion controlled boundary migration were considered by Furu et al.: (i) the pure metal case; $V_a=b^3$ and $U_a\equiv U_{SD}$ (i.e. self diffusion), and (ii) the solute pinning case; $V_a=\omega_b b^3 c^{-1}$ (ω_b is a geometrical constant) and $U_a=U_s$. In the first case $PV_a<<kT$ and Eq. 12 can be solved analytically giving the following growth law

$$\frac{\delta}{\delta_0} = (1+\frac{t}{\tau_3})^{1/2} \qquad (14)$$

where

$$\tau_3 = \left[0.04 v_D B_\delta (\frac{b}{\delta_0})^2 (\frac{Gb^3}{kT})\exp-\frac{U_{SD}}{kT}\right]$$

In the case of solute pinning, PV_a may be larger than kT and Eq. 13 needs to be solved numerically.

2.3 Recrystallization kinetics

The recrystallization kinetics are calculated by a standard Avrami equation of the following form:

$$X(T,t) = 1-\exp-(\frac{t}{\tau_r})^n \qquad ,\tau_r = \tau_r^0 \exp\frac{U_r}{kT} \qquad (15)$$

where U_r is the activation energy for recrystallization (i.e. migration of a high angle grain boundary), τ_r^o is the pre-exponetial of the relaxation time for recrystallization and n is the Avrami exponent.

3 APPLICATION OF THE MODEL

3.1 Recovery in AlMg alloys

Aluminium-magnesium alloys combine an appreciable solute solubility with a strong solute-retarding-effect on dislocation mobility. This provides the technological bases for the important 5000-series AlMg-alloys, of which a most characteristic feature is their capacity for strain hardening. By cold rolling reductions typical of commercial sheet production (ε≈1-2) the yield stress can be more than tripled, compared with the fully soft condition, e.g. an Al-4wt% Mg alloy cold rolled to strain of about ε=1.5 (H18) will have a yield stress of about 300 MPa or more, compared to the fully soft flow stress of around 100 MPa. TEM examination of heavily strained AlMg-alloys accordingly reveals a very high, and apparently uniform distribution of dislocations. Another characteristic aspect related to the mechanical properties of cold worked AlMg-alloys pertains to their recovery behaviour. Strain hardened AlMg-alloys recover much more rapidly than other wrought aluminium alloys. Further, as mentioned in the introduction, in AlMg-alloys recovery

can even be followed at room temperature, Fig. 2a-c. Figure 2c indicates that the recovery rate appears to be independent of the amount of initial cold deformation. However, this is only seemingly so, if the data in Fig. 2a-c are re-plotted as fraction retained strain hardening *R vs log t* it becomes quite clear that the recovery rate increases with decreasing rolling reduction, and for a given reduction, increases with increasing additions of magnesium, Fig. 5a.

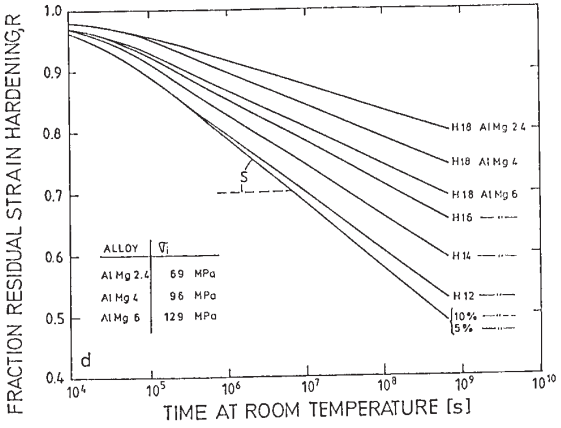

(a)

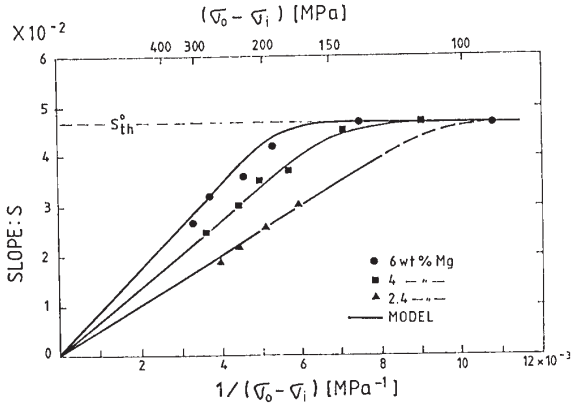

(b)

Fig. 5 a) The same results as in Fig. 2 plotted as *R vs t*. b) The slope of the curves in a) as a function of the inverse of the initial strain hardening *(1/(σo - σi))*.

The 17-year long Alcoa study has resulted in a remarkable set of data which recently have been subjected to a detailed analysis by Nes [5]. As these results clearly document that the recovery in mechanical properties follows a logarithmic decay, Nes applied the model presented in Section 2.1 in order to reveal the details of the mechanism controlling the network growth reaction. At room temperature, the contribution to the recovery of the flow stress due to subgrain growth can be safely ignored and Eq. 2 takes the form: $R=1+f_1(\sqrt{(\rho_i/\rho_{io})}-1)$ which in combination with Eq. 9 gives:

$$R = 1 - S_{th} \ln(1 + \frac{t}{\tau_1}) \qquad (16)$$

where the slope parameter $S_{th} = (f/(1_a\sqrt{\rho_{io}}))(kT/Gb^3)$. This slope parameter can be expressed in two different ways, depending on the amount of deformation prior to annealing:

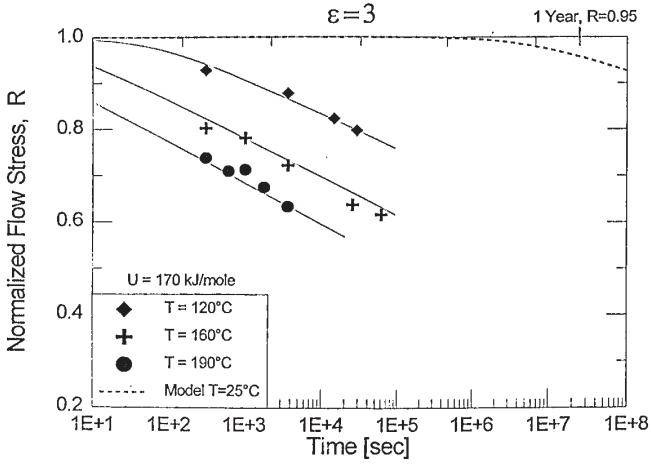

Fig. 6. Fractional residual strain hardening as a function of annealing time at the temperatures given, experimental data from Barioz et al. [17].

(i); At small strains (typically 10 % or less) a characteristic aspect of work hardening is microstructural scaling (or similitude), under which conditions the fractional flow stress contribution, f, becomes a constant ($f=f_{sc}$), and since $\sqrt{\rho_{io}} = f_{sc}\sqrt{\rho_o}$ the slop-parameter can be written $S_{th} = [l_j(\sqrt{\rho_o})(kT/Gb^3)]^{-1}$. (ii); At large strains (stage III or IV) $f = \alpha_1 MGb\sqrt{\rho_o}/(\sigma_o - \sigma_i)$ and the slope parameter becomes $S_{th} = (\alpha_1 MkT/(l_a b2))(\sigma-\sigma_i)^{-1}$.

It is interesting to compare these theoretically predicted slopes to the experimentally observed ones (Fig. 5a), i.e. to compare the variation in slope as a function of $(\sigma_o-\sigma_i)^{-1}$. Such a S_{exp} *vs* $(\sigma_o - \sigma_i)^{-1}$ plot is shown Fig. 5b. Firstly, it is noted that for each alloy the slope S varies linearly with $(\sigma_o - \sigma_i)^{-1}$ up to a critical value S_o, after which it remains constant for increasing values of $(\sigma_o - \sigma_i)^{-1}$, or decreasing rolling reductions. This observation opens for some interesting interpretations in terms of the mechanisms controlling the jog separation as discussed above, i.e. in terms of Eqs. 11 and 12. During annealing following heavy cold rolling the jog separation will be controlled by the solute content according to Eq. 11. Under such conditions the slope parameter will depend on both the solute content and the initial flow stress as follows:

$$S_{th} = \frac{\alpha_1 MkT}{\omega_s b^3} c^e (\sigma - \sigma_i) \qquad (17)$$

However, under conditions where the initial cold reduction is less than 10% (i.e. microstructural scaling applies) Eq. 12 defines the jog separation and the slope parameter becomes a constant defined as follows:

$$S_{th}^0 = \frac{C}{\omega_j}\left(\frac{kT}{Gb^3}\right) \qquad (18)$$

It is interesting to note that these model predictions are fully consistent with the experimental observations as illustrated in Fig. 5b where the parameters involved have been given the following values: $e = 0.6$, $\omega_s = 3.5$ and $\omega_j = 14$, all reasonable values, indeed.

The annealing behaviour of heavily deformed AlMg alloys at temperatures below 200°C has been studied by Barioz et al. [17], and their results for an Al3Mg alloy deformed to a strain of 3 prior to annealing is analysed in terms of the present model in Fig. 6. As can be seen from this figure the experimental results are well accounted for by selecting an activation energy of 170 kJ/mol, which is a reasonable value [18]. Also note that the model prediction is that this alloy, in the condition investigated, will recover to 95% of its original strength in one year, a reasonable result compared to the Alcoa investigation, bearing in mind the much higher rolling reduction of the alloys modelled in Fig. 6.

3.2. Subgrain growth in heavily deformed alloys

Subgrain growth is the least well characterized and understood recovery reaction. During annealing following small pre-strains, Young et al. [7] observed that the cell/subgrain structure coarsened due to a coalescence mechanisms (annealing temperatures in the range 120-200°C). For pre-strains in the range 15% - 25% virtually no coarsening of the subgrain structure could be detected during annealing in the same temperature range, even though the initial cell size for these strains were considerably smaller. The main changes in the boundary structure, comparing different pre-strains, pertain to that at strains less than 15% the boundary misorientation was small, only 0.3°, while for strains larger than 15% this misorientation increases linearly with strain reaching about 0.7° at a strain of 25%. As the boundary misorientation increases the importance of the coalescence reaction appears to decrease. It was interesting to note that Gleiter [15] reported that in an AlCu alloy cold rolled to a 90% reduction and annealed in situ the coarsening reaction was controlled by sub-boundary migration, except for boundaries of small misorientations (<0.3°), which were observed to dissolve. So the conclusion becomes that in heavily cold deformed aluminium ($\varepsilon>1$) subgrain growth is dominated by boundary migration.

Subgrain growth is modelled in Section 2.2. Compared to the classic climb based treatment by Sandström [11,13,16], the new aspect introduced by Furu et al. [2] is that also in the case of sub-boundary migration the activation volume involved may reach such values that PV_a (see Eq. 13) becomes comparable to, and even larger than, kT. The observations by Furu et al. from subgrain growth in a commercial purity alloy (AA 1050) have recently been re-analysed by Sæter [19] with the result shown in Fig 7a and b. Since these subgrain size data are indirect ones, derived on the basis of hardness measurements, Sæter, in addition, performed a detailed TEM investigation of subgrain growth in a commercial purity alloy of a slightly different composition (AA 1070), the result of which is presented in Fig. 7c and d. These two sets of experimental observations are analysed both in terms of a simple climb-based mechanism, Fig. 6a and c, and in terms of a solute pinning mechanism, Fig. 7b and d. The pure climb-based mechanism which predicts a parabolic growth law, Eq. 14, seems to apply at temperatures above 300 °C, but fails at lower temperatures. Solute pinning. on the other hand (Eq. 13 with $PV_a > kT$), applies very well in the low temperature regime, but not so well at temperatures above 300°C. The high temperature solution requires in both cases an activation energy of 125 kJ/mol, which is typical of self diffusion in aluminium, while the solute pinning solutions are, in both cases, based on an activation energy of 194 kJ/mol. This latter activation energy is of the same size as that for diffusion of iron in aluminium. In the case of solute pinning the activation volumes involved are $2.8*10^3\ b^3$ and $6.3*10^3\ b^3$ for the 1050 and 1070 alloys respectively. Before discussing this change in activation energy more in detail, another set of experimental subgrain growth data will be presented.

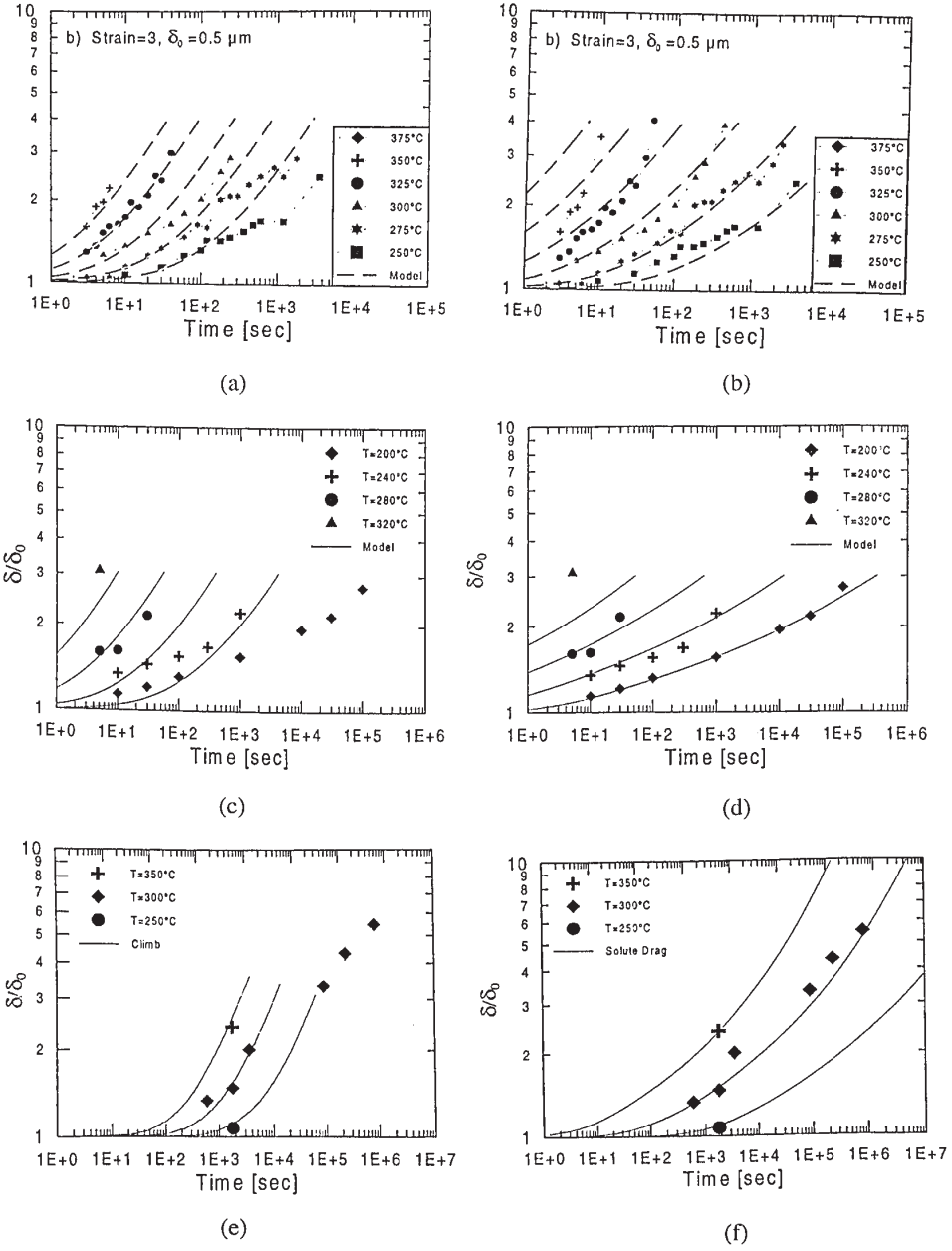

Fig. 7. Normalised subgrain size vs time during isothermal annealing at the temperatures given. Experimental observations and modelling predictions. a-b) alloy 1050 [2], c-d) alloy 1070 [19] and e-f) an Al0.05Si alloy [20].

A main problem in studying subgrain growth is the very limited size span which can be obtained, usually less than a factor two, because of the interference of recrysrallization. In a very recent investigation of normal and abnormal subgrain growth in an Al-0.05Si alloy by Ferry and Humphreys [20], this problem has been overcome. The Ferry and Humphreys results, Fig. 7e and f, are of extraordinary quality as being the only one available which spans almost a factor 10 in the subgrain size range. Their results are in Figs 7e and f analysed in a similar way to that above, i.e. in terms of a parabolic growth law or due to solute pinning. Ferry and Humphreys followed the subgrain growth reaction for nearly 300 hours at 300°C. However, only during the first 3 hours, the parabolic growth can be applied, Fig. 7e, the activation energy of which is 90 kJ/mole, which is a very low value compared to that of self diffusion in aluminium. An interpretation in terms of solute pinning, on the other hand, gives a much better fit to the experimental data as shown in Fig, 7f. In the latter case the activation energy becomes 192 kJ/mol and the activtion volume $1.4*10^4\ b^3$.

It follows from this subgrain growth analysis that a parabolic growth law does only apply at temperatures above 300°C. At lower temperatures it has been demonstrated that a solute pinning mechanism gives an adequate representation of the growth kinetics. The question then becomes: what is the reason for such a transition? An interesting speculation is that this transition in growth kinetics is caused by precipitation, or cluster formation, associated with iron atoms in supersaturated solid solution. A condition for such an interpretation becomes that the sub-boundaries are able to unpin themselves from the clusters by thermal activation. By increasing the temperature, such clusters are no longer stable and the kinetics revert to being climb controlled. The sizes of the activation volumes involved are consistent with such a cluster-mechanism. These activation volumes corresponds to the following iron contents in solid solution; 350 ppm, 160 ppm and 70 ppm respectively for the 1050, 1070 and the alloy investigated by Ferry and Humphreys. The iron contents in the two commercial purity alloys have, on the basis of phase diagram calculations and resistively measurements been estimated to be: 380 ppm for the 1050 alloy and 230 ppm for the 1070 alloy.

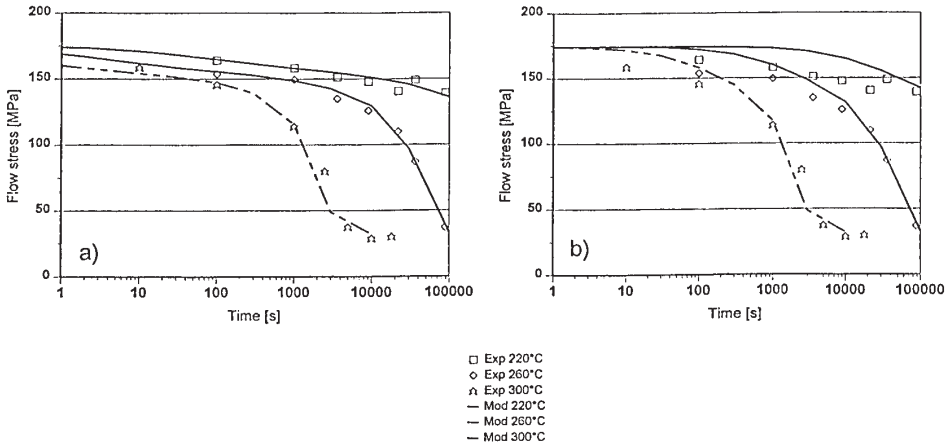

(a) (b)

Fig. 8. Model predictions compared with experimental data of alloy 1050: a) model including subgrain growth and annihilation of internal dislocations, b) model including only subgrain growth.

3.3 Modelling industrial back annealing

Most of the softening during industrial back annealing of hot line processed 1xxx- and 3xxx alloys takes place at temperatures so low that the solute pinning mechanism developed above is expected to control the subgrain growth reaction. Under such conditions back annealing is modelled by combining Eq. 3 with Eqs. 8, 13 and 15. The application of such a model to the back annealing of 1xxx- and 3xxx alloys are covered in a special presentation at this conference [21], and an example of the prediction power of this approach applied to an 1050 alloy is illustrated in Fig. 8a. Although recovery in this type of alloys is dominated by the annealing behaviour of the subgrain structure, the annealing out of the internal dislocations cannot be ignored as illustrated by Fig. 8b.

ACKNOWLEDGEMENT

The authors wish to acknowledge Hydro Aluminium for financial support.

REFERENCES

[1] M. Cook and T.L. Richards: J. Inst. Met., 73, (1946), 1-31.
[2] T Furu, R. Ørsund and E. Nes:Ø Acta Met. et Mater., 43, (1995) 2209.
[3] E.H.Dix, W.A. Anderson and M. Byron Shumaker: Corrosion, 15, (No. 2) (1959) 19.
[4] R.E. Sanders, S.F. Baumann and H.C. Stumpf: Non-Heat-Treatable Aluminium Alloys. Int. Conf. Aluminium Alloys (ICAA1) (University of Virginia, Charlottesville) (1986) p.1441.
[5] E. Nes: Acta Met. et Mater., 43, (1995), 2189.
[6] E. Nes and J.A. Sæter: Proc. 16th Risø Int. Symposium on Materials Science, Editor N. Hansen et al. Roskilde (1995), 169.
[7] C.T. Young, T.J. Headley and J.L. Lytton: Materials Sci. Eng., 81, (1986) 391.
[8] B. Forbord: PhD-thesis, NTNU, Tronheim (1999).
[9] J. Friedel: Dislocations, Addison-Wesley, London, (1964), p. 277.
[10] J.C.M. Li: J. Appl. Phys., 33, (1962), 2958.
[11] R. Sandström: Acta Met., 25, (1977), 897.
[12] R.D. Doherty and J.A. Szpunar: Acta Met., 32, (1984), 1789.
[13] R. Sandström, B. Lehtinen, E. Hedman, I. Groza and S. Karlsson: J. Met. Sci., 13, (1978), 1229.
[14] A.R. Jones, B. Ralph and N. Hansen: Proc. R. Soc. A368, (1979), 345.
[15] H. Gleiter: Phil. Mag. 20, (1969),821.
[16] R. Sandström: Acta Met., 25, (1977), 905.
[17] C. Barioz, Y. Brechet, J.M.Legresy. M.C. Cheynet, J. Courbon, P. Guyot and G.M. Raynaud: 3rd. Int. Conf. on Aluminium Alloys (ICAA3), The Norwegian Institute of Thechnology, Trondheim (1992), 347.
[18] D. Altenpohl: Aluminium und Aluminiumlegierungen, Springer-Verlag, Berlin (1965), 536.
[19] J.A. Sæter: PhD-thesis, Trondheim (1997).
[20] M. Ferry and F.J. Humphreys, Acta mater. 44, (1996), 1293.
[21] H.E. Vatne, T. Furu and E. Nes: (ICAA6), this conference (1998).